EMG-driven Machine Learning Control of a Soft Glove for Grasping Assistance and Rehabilitation.

Marek Sierotowicz[1†*], Nicola Lotti[2†], Laura Nell[2], Francesco Missiroli[2], Ryan Alicea[2], Xiaohui Zhang[2], Michele Xiloyannis[3], Rüdiger Rupp[4], Emese Papp[5], Jens Krzywinski[5], Claudio Castellini[1‡] and Lorenzo Masia[2‡]

***Abstract*— In the field of rehabilitation robotics, transparent, precise and intuitive control of hand exoskeletons still represents a substantial challenge. In particular, the use of compliant systems often leads to a trade-off between lightness and material flexibility, and control precision. In this paper, we present a compliant, actuated glove with a control scheme to detect the user's motion intent, which is estimated by a machine learning algorithm based on muscle activity. Six healthy study participants used the glove in three assistance conditions during a force reaching task. The results suggest that active assistance from the glove can aid the user, reducing the muscular activity needed to attain a medium-high grasp force, and that closed-loop control of a compliant assistive glove can successfully be implemented by means of a machine learning algorithm.**

I. Introduction

One of the most visionary philosophers of the current century stated that without our hands *"...we are, are we not, nothing but naked apes..."* [1]: indeed, this complex of multi-joint articulations is crucial to perform most tasks of daily living [2]. Moreover, the hands play a very important role in non-verbal communication.

Unfortunately, neuromuscular diseases and traumatic events that impair manipulation skills have significant incidence rates, and can dramatically worsen the quality of life for affected people [3]. When the technology reached a sufficient level of maturity, wearable robotics entered the stage to help people with motor impairments in restoring or compensating for lost motor functions [4]: in particular, the introduction of soft materials in these actuated devices enhanced the human-machine interaction with promising results in the rehabilitation realm [5], [6], [7].

Most of the soft actuated gloves present in literature are controlled based on intent detection algorithms, but many aspects are still challenging [8]: the most common approach is based on motor synergy analysis, which can simplify the otherwise prohibitively complex mapping of muscle activity to primary postural tasks [9]. This is done by identifying specific patterns in brain activity [10], [11] or neuromuscular signals [12], [13], [14], [15]. The latter approach has been further developed by Polygerinos and colleagues, who introduced a control based on surface electromyography (sEMG) of a pneumatic system [16]: the open-loop sEMG logic classified gross muscle contractions responsible for flexion and extension and fed the information to a low-level fluid pressure controller which regulated the pressure simultaneously in all actuators of a pre-selected group. Another example can be found in Bos et al. [17], who developed the sEMG-based control algorithm for the SymbiHand: the muscle activity was mapped into a grasping force and served as input for the actuation stage.

In prosthetic control, and generally when controlling hand-emulating robotics by means of sEMG, machine learning (ML) has been used with a good rate of success [18], [19], [20]. The main advantage of such predictive algorithms is the fact that they do not require explicit mapping of muscle activity to hand movement or posture, and that they can fit each individual user. The main disadvantage is the computational cost that these algorithms can require, especially during training, and the fact that they sometimes have unpredictable responses, especially when the user deviates from the conditions present during training. An example is the so-called limb position effect, which describes changes in muscular activity associated to a single hand posture when the upper limbs assume different postures and consequently muscle recruitment varies [21]. These downsides represent the main obstacles for the use of these control systems outside of clinical settings. Nevertheless, solutions have been proposed, which, while using very simple machine learning algorithms, still allow for robust control of prosthetic devices [22].

In our previous study [23] we demonstrated how an open-loop kinematic synergy-based control in combination with a soft assisting glove can provide assistance in the presence of grasp weakness. Starting from our previous work regarding both the topic of exosuits and ML-based prosthetic control, here we combine, for the first time, a soft wearable glove with a user's motion intent detection based on machine learning approaches enrolled in a closed-loop architecture. The device is characterized by means of a rehabilitative

† M. Sierotowicz and N. Lotti equally contributed to this work.

‡ L. Masia and C. Castellini equally contibuted to this work.

[1]M. Sierotowicz and C. Castellini are with the Institute of Robotics and Mechatronics, German Aerospace Center (DLR), 82234 Wessling, Germany and with the Department of Artificial Intelligence in Biomedical Engineering (AIBE), Friedrich-Alexander-Universität Erlangen-Nürnberg (FAU), 91052 Erlangen, Germany.

[2]N. Lotti, L. Nell, F. Missiroli, R. Alicea, X. Zhang and L. Masia are with the Institute for Technical Informatics (ZITI), Heidelberg University, 69120 Heidelberg, Germany.

[3]M. Xiloyannis is with the Institute of Robotics and Intelligent Systems, ETH Zürich, Zürich, 8092, Switzerland.

[4]R. Rupp is with the the Spinal Cord Injury Center of Heidelberg University Hospital, 69120 Heidelberg, Germany.

[5]E. Papp and J. Krzywinski are with the Chair of Industrial Design Engineering, Technical University of Dresden, 01062 Dresden, Germany.

[*] corresponding author, marek.sierotowicz@dlr.de

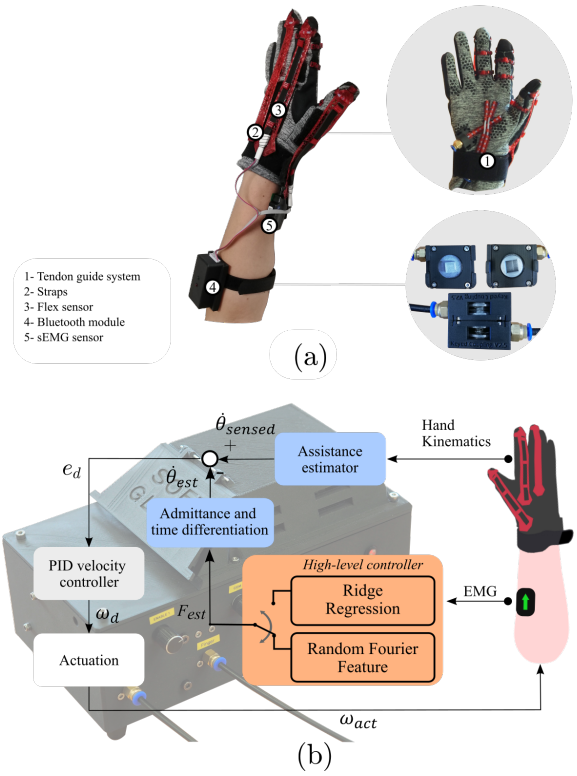

Fig. 1. *MyoGlove design and control.* **a**: the presented prototype actively assists hand grasping by means of tendon-driven actuators (1) lodged in the driver's stage. Hand opening is passively aided by three 3D printed elastic straps integrated in the glove (2). Hand movements are sensed by means of two flex sensors connected to a Bluetooth data collection module measuring overall thumb and index flexion/extension (3-4). The motion intent is estimated by means of sEMG (5). A magnetic clutch has been developed in order to allow for quick (de)coupling of the glove from the driver stage allowing for quick adjustments to the user's hand size (visible in the lower right corner of **a**). **b**: block diagram depicting the control architecture of the MyoGlove. The high-level controller aims to estimate the intended grasping force through a ridge regression or a random Fourier features algorithm. This estimate is then converted to an intended displacement through the admittance of the handle device. The first time derivative of the displacement is used as set-point and compared with the angular velocity measurement of the flex sensors in the low-level PID controller which translates the tracking error into a motor angular velocity, which is finally converted into an actuation command.

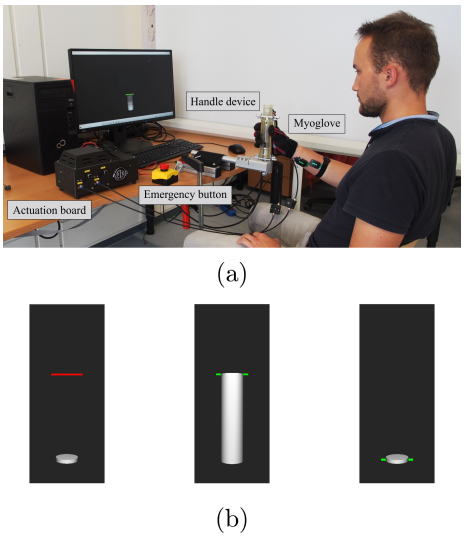

Fig. 2. *Setup and task description.* **a**: experimental setup with a participant. **b**: screenshots representing the task as shown to the user over the GUI. The red line highlights the target force to be reached. When the participant exerts a level of force within the threshold from the target, the line is highlighted in green, and subsequently reset to the starting level.

apparatus that includes a haptic handle device for grasping training. We investigate, by comparing two different machine learning algorithms, the kinematic and physiological effects of the glove in a cohort of six healthy users, in a repeated-measures study design. The machine learning algorithms used in this study had already found ample use in our previous work on the control of rigid prosthetic devices [22]. The results provide initial indicators for the usability of this apparatus in rehabilitation for task-oriented restorative training.

II. MyoGlove Design

The control algorithm has been tested on a two degrees of actuation glove able to assist flexion of index and middle finger, and flexion of the thumb, respectively, by means of a tendon-driven system (Fig. 1a). The tendons are routed at the palm of the hand using a sewn-on guiding system, consisting of Teflon tubes held in place by 3D-printed parts. These lead the tendons around the fingertips of the assisted fingers in order to get a better distributed pulling force, to end up in a Bowden cable system (Shimano, SLR, $\varnothing 4\,\mathrm{mm}$, Sakai, Õsaka, Japan), starting at the proximal end of the palm and terminating on a pulley lodged in a case which can be magnetically secured to a clutchable customized 3D-printed system (Fig. 1a). This design allows to easily connect gloves of different sizes to the actuation stage (visible in Fig 1b). Besides the active assistance of flexion movements, extension is passively aided through 3D-printed elastic straps mounted as shown in Fig. 1a. Whenever extension intent is sensed and the motors release the tendons, the straps assist the fingers in extending, acting as antagonistic muscles. Two flex sensors (Bend Labs, Salt Lake City, UT, USA) are attached to the straps at the index and thumb to detect their overall bending angle during flexion and providing position feedback to the low-level control loop. Two movements, namely flexion of the thumb and flexion of the fingers, are independently assisted by motors which pull and release the respective tendon cable. The actuation stage is placed in a custom-designed box (Fig. 1b and in Fig. 2 a), which contains the two brush-less electric motors (T-Motor 6007,Nanchang, Jiangxi, China), the motor driver unit (ODrive v3.6, ODrive robotics, San Jose, CA, USA), and the electronics needed for data processing and transmission. The communication with the motors is handled by an Arduino Mega 2560 (Arduino, Ivrea, Italy), which also receives the data from the flex sensors using Bluetooth low-energy protocol through dedicated boards (nRF52832 Bluefruit Feather, Adafruit,

New York, NY, USA) and furthermore hosts the low-level control loop. The high-level control model, implemented using Matlab/Simulink environment (MathWorks, Natick, Massachusetts MA, USA), runs on a Nvidia Jetson Nano board which receives and processes the EMG data and sends back the calculated motor commands to the Arduino, which forwards them to the motor drive unit using serial protocol. Muscular activity is measured by means of two sEMG sensors (Delsys Trigno, Natick MA, USA) placed on the flexor digitorum (FD) and the abductor pollicis brevis (APB) muscles, by following the SENIAM guidelines [24].

III. Real-time control architecture

In the present work, besides characterizing the system, we also aimed at comparing the performance of the two main intent estimators, which are both based on machine learning. For the sake of clarity, the two approaches worked in a mutually exclusive manner, being tested separately and across distinct trials, but being used by all participants.

As depicted in Fig. 1b, the architecture comprised a high-level controller, based on one of the two approaches (selected prior to test initiation), which estimated the motion intent and thus computed the set-point for the low-level admittance controller. This last layer was used in both conditions and was implemented to track the reference signal and convert it into a motor actuation command closing the loop on the flex sensors measurements (100Hz, LP filter at 10Hz).

A. High-level control layer: machine learning-based estimation

The two intent estimators consisted of a non-kernelized *ridge regression* algorithm applied directly to the filtered sEMG envelopes (sampled at 2kHz, BP filtered between 35Hz and 350Hz, rectified, LP filtered at 4Hz), and in a *random Fourier features* kernelized algorithm, respectively. Both the approaches aimed to estimate a grasping force (F_{est} in Fig. 1b). This was then converted into a finger displacement θ_{est} through an admittance consisting of a task-specific compliance determined by the the handle device. This displacement θ_{est} was fed as input to the low-level controller after first order time differentiation, as described in Sec. III-B and shown in Fig. 1b.

1) Ridge regression algorithm: ridge regression (*RR*) is among the most fundamental algorithms used in machine learning [25]. It has computational complexity of $\mathcal{O}(DC)$ (D and C being the number of observed features and the number of output channels, respectively) for the prediction step and, being a linear model, it is typically not prone to overfitting. The necessity to work with a matrix with a dimension equal to the number of observations at training time represents the main computational cost for this algorithm, which is $\mathcal{O}(D^3 + D^2N)$ at training time (N being the number of observations, and typically $N \gg D$). However, this operation can be carried out incrementally by means of the Sherman-Morrison formula [22] [26] thus reducing the overall complexity at training to $\mathcal{O}(D^2)$ for every new observed sample. This can be especially useful for higher dimensionality D, which can be necessary when applying a higher-dimensional kernel mapping. (see section III-A.2). The Sherman-Morrison formula enables an efficient implementation of incremental learning, where the predictor can efficiently integrate new data into the design matrix, thus enabling the user to adjust to changing conditions which might influence the prediction, such as varying levels of perspiration or fatigue.

2) Random Fourier Features algorithm: Random Fourier features (*RFF*) make it possible to add an approximated radial basis function kernel without losing the incremental character of non-kernelized *RR* [27], [28]. A kernel allows the model to better adapt to non-linearities and has been shown to offer better performance in prosthesis control when training a model to identify forces on multiple degrees of freedom [22]. On the other hand, it is more prone to overfitting if its hyperparameters are not suitably tuned. Furthermore, it entails an increase in feature dimensionality, meaning that D increases.

B. Low-level controller: position-velocity loop

As the low compliance from the cables made it difficult to open one's hand once a grasp was achieved, the control was closed around the error in the first time derivative of the finger flexion angle $\dot{\theta}$.

The actuation to the glove is thus controlled in a closed loop around the error between the desired set-point $\dot{\theta}_{est}$ provided by the machine learning algorithm through the known admittance of the handle device and the measurements from the flex sensors $\dot{\theta}_{sensed}$ normalized through a calibration procedure. The resulting instantaneous velocity tracking error $e_d = \dot{\theta}_{sensed} - \dot{\theta}_{est}$ is transformed into a desired angular velocity, ω_d, through a PID block of the form:

$$Y(s) = \frac{\omega_d}{e_d} = \frac{K_p + K_i \cdot s^{-1}}{1 + K_d \cdot s} \tag{1}$$

where the K_p, K_i and K_d gains were experimentally tuned, using the Ziegler-Nichols heuristic method [29], prior to the study and then left unchanged for all participants.

As mentioned above, in order to calculate the error e_d, the grasp force estimation from the machine learning algorithm and the bending sensor feed were projected onto a common space through an admittance (or compliance) gain and a normalizing factor, respectively, as illustrated in Fig. 1 b. The normalizing factor was obtained during a calibration procedure prior to session start during which the experimenters gathered the values output by the flex sensors while the user had their hand open and closed. The admittance, on the other hand, is fixed as the inverse of the handle's impedance, as explained in Section IV-A. Both signals were then differentiated over time before being fed to the aforementioned PID motor controller.

IV. Experimental setup and protocol

Six healthy participants were enrolled in the experiment (4 males/2 females, age 26.17 ± 1.33 years, body weight

$80.33 \pm 13.29\,\mathrm{kg}$ and height $1.80 \pm 0.11\,\mathrm{m}$, mean $\pm$ sd). Inclusion criteria were based on no evidence or known history of musculoskeletal or neurological diseases, and exhibiting normal joint range of motion and muscle strength. All experimental procedures were carried out in accordance with the Declaration of Helsinki on research involving human subjects and were approved by the IRB board of Heidelberg University (Nr. S-311/2020). All subjects provided written informed consent to participate in the study.

A. Apparatus

In order to test the *MyoGlove* controllers' performance, we developed a customized setup that could be used in future studies for rehabilitation treatments: we combined the device with an actuated hand module [30] aimed to provide haptic feedback (Fig. 2a, handle device). An impedance controller was implemented in order to generate a constant-compliance force field during grasping. The handle's force F^h is related to the finger and manipulandum displacement according to the following equation,

$$F^h = K\Delta r = C^{-1}\Delta r \tag{2}$$

where $K = 1\,\mathrm{kN/m}$ is the stiffness gain and Δr is the handle displacement, obtained from the outer and inner rotors, as reported in [30], C is the compliance gain, which corresponds to the inverse of the stiffness gain. All of the gains were assumed to be constant in this experiment.

A DAQ board (Quanser QPIDe, Markham, Ontario, Canada) mounted on a dedicated desktop workstation was used to control the handle device and acquire all its signals, with a sampling frequency of $1\,\mathrm{kHz}$ (Fig. 2a). The workstation provided visual feedback to the user.

B. High-level controller calibration

Before starting the experiment, both high-level control algorithms (i.e. *ridge regression* and *random Fourier features*) were trained on a common dataset acquired during a separate round which also served for familiarization. This dataset is specific to each user and electrode placement, and therefore the acquisition round took place immediately prior to the session proper. During the acquisition, participants had to follow a visually fed back preset force profile by grasping the handle device (Fig. 2b). The force profile was then used to associate target labels $F^h \in \{0\,\mathrm{N}, 5\,\mathrm{N}, 10\,\mathrm{N}, 15\,\mathrm{N}\}$ to the acquired sEMG envelope signals in order to train the two machine learning algorithms.

The algorithms were each trained on a set of measurements from the two EMG probes (therefore each observation had 2 features) acquired at a rate of $1\,\mathrm{kHz}$ over a time of $10\,\mathrm{s}$ per label, with 5 repetitions, for a total of ca. 50000 samples per target force. The prediction was verified in terms of correlation of the estimated applied force against the target force level, and if needed, data acquisition was repeated, until the output results showed good correlation with the force profile and no apparent noise due to overfitting. The main source of errors in the prediction at this stage was bad placement of the EMG probes, which, if found, was corrected.

Both RR and RFF have a deterministic closed form solution. Furthermore, the main purpose of the implementations of RR and RFF we use is to facilitate incremental learning, which is to say that the user should be able to easily and efficiently add new samples on the fly in order to obtain better generalization. To this end, the algorithm's hyperparameters are to remain constant throughout usage [22]. These were set experimentally prior to the main experiments. Therefore, two of the experimenters tested the algorithms with different values for the hyperparameters and selected the ones which gave the better results in terms of generalization. As all hyperparameters were preset and the algorithm's optimization is deterministic, no validation round was conducted prior to the individual experimental sessions.

C. Comparison task

The main test consisted in a repeated-measure force reaching task in which participants, wearing the glove, were prompted by a GUI to reach four different isometric grasp force steps ($F^h \in \{0\,\mathrm{N}, 5\,\mathrm{N}, 10\,\mathrm{N}, 15\,\mathrm{N}\}$), grasping the handle device (Fig. 2a).

The participants' grasping force was visualized in the monitor as a white bar, which changed according to the force level. The target force step, instead, was represented via a horizontal line that changed color based on the condition (Fig. 2b): when the user was in the *rest* condition (i.e. $F^h = 0\,\mathrm{N}$), a new target force, displayed as a red line (Fig. 2b, left), appeared on a predefined level of the screen based on desired force intensity. Participants had to increase their grasp force on the handle device until the desired level was reached: once it was reached, the line changed its color from red to green (Fig. 2b, centre) and the grasp force had to be maintained for $2\,\mathrm{s}$. After this, the red line returned to the rest condition (i.e. $F^h = 0\,\mathrm{N}$) and participants were instructed to relax for $2\,\mathrm{s}$, until a new force target appeared (Fig. 2b, right). The whole sequence of force step was repeated a total of 5 times for each non-zero target force value.

The task was repeated in three different conditions: (i) without providing glove assistance (i.e. *NA* condition), (ii) with the *ridge regression* algorithm (i.e. *RR*) and (iii) with the *random Fourier feature* algorithm (i.e. *RFF*). The sequence of force steps and conditions were randomized for each participant and condition in order to account for order effects (fatigue, learning), when averaging across participants.

V. Data analysis

Offline analysis was performed to evaluate participants performance under active assistance (RR and RFF) compared to the *NA* condition. Outcome measures included prediction accuracy, motor actuation response, and changes of muscular activities. Furthermore, the performances of the *RR* and *RFF* algorithms were directly compared in terms of R^2 score and Root Mean Square Error (RMSE). We used an external

trigger to synchronize the DAQ board and the glove control unit during data processing and analysis.

A. Prediction accuracy

In order to quantify the controllers' reliability in estimating the force at the end-effector, we compared the grasping force performed during *NA* condition with the *RR* and *RFF* offline predictions using the EMG data acquired during the trial as input. We evaluated the correlation coefficient R^2 and RMSE between the measured and the predicted force levels from the early onset of the grasp movement until the end of the holding phase.

B. Motor actuation response

In order to evaluate the system's response time, we employed cross-correlation between the recorded sEMG envelope and the motor response recorded through the motor's positional encoder when the participant started applying the force necessary to reach the target grasp force.

C. Changes in muscular activity

Electromyographic signals of APB and FD were post-processed offline through a band-pass filtering (35 Hz-350 Hz) with a second-order Butterworth filter, full wave rectification, a low-pass filtering (4 Hz, second-order Butterworth filter) and normalized to the highest value of each participant during the whole experiment (i.e. MaxEMG).

We then used the root mean square (RMS) of the sEMG envelope as index of activation level across force steps (i.e. 5 N, 10 N and 15 N) and assistance conditions (i.e. *NA*, *RR*, *RFF*).

D. Statistical analysis

Data normality distribution was assessed using Shapiro-Wilk test, and sphericity condition for repeated measures analysis of variance (rmANOVA) was assessed using the Mauchly test. The rmANOVA test was used to examine the effects on the dependent variables of the assistance type, using it as within-subject factor (it can assume one out of 3 levels: *NA*, *RR*, *RFF*). A post-hoc analysis was performed using paired t-tests to evaluate the significant pairwise differences between each type of assistance for the different force steps (3 levels of F^h: 5 N, 10 N, 15 N). For all the tests, the level of statistical significance was set at 0.05, except for post-hoc analysis, where the significance level was chosen according to the Bonferroni correction for multiple comparisons.

VI. Results

A. Both controllers have a good prediction accuracy

The first outcome metrics have the purpose of evaluating the performance of the two controllers in terms of motion intent prediction: Fig. 3a shows the mean R^2 coefficients over model and target force. The R^2 scores average overall was 0.8009 ± 0.1665 for the *RR* condition and 0.7303 ± 0.2295 for the *RFF* condition, respectively.

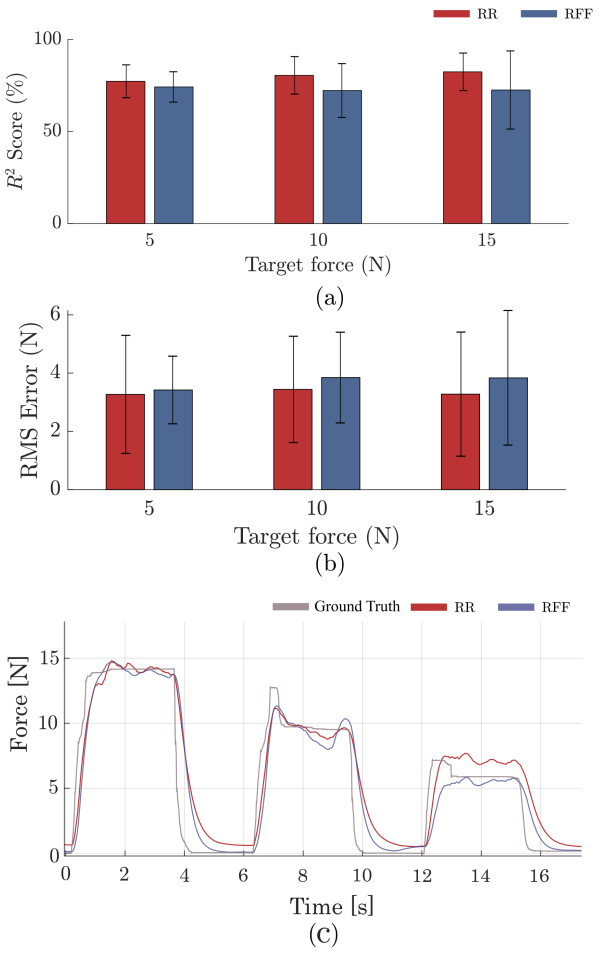

Fig. 3. **a**: R^2 values for *RR* and *RFF*. **b**: RMS Error w.r.t. the measured force. **c**: representative grasp force prediction vs. measured grasp force.

It is however worth mentioning that the R^2 score computed between the EMG envelopes and the actually produced force shows comparable values (0.7848 ± 0.1684).

The Root Mean Square Error (RMSE) was calculated over the same motion phases. Fig. 3b shows its values over model and target force. Overall, RMSE was 3.3293 ± 1.9771 N for the *RR* condition and 3.7010 ± 1.7328 N for the *RFF* condition.

Fig. 3c shows a representative plot of grasp prediciton vs. the actually measured force at the handle. A noteworthy effect is that, in certain portions of the plot where the measured force does not appear to change, both predictions show noticeable instability (for example between 8 s and 10 s). The most obvious explanation for this effect is the presence of static frictions in the handle device, which would cause the mechanism to remain static even if the force applied by the user's muscles changes somewhat. This is, of course, a potential source of RMS error.

B. The system shows an overall small delay

The time between the neuromuscular signal and the motor actuation is an important metric related to the system's

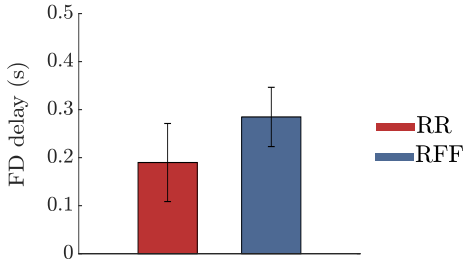

Fig. 4. Motor actuation delay across all subjects.

reactivity. Because the control loop does not explicitly map the APB sEMG with the thumb motor or the FD sEMG with the finger motor, cross correlation was computed for all four possible sensor-motor correlation, and only the smallest delay was considered, operating on the assumption that the motor moving was caused by the nearest increase in muscle activity. Apparently non-causal behavior was excluded from the calculation. Fig. 4 depicts the results of the cross-correlation between the muscle activities and the corresponding motor's encoder. No significant difference was found between the two controllers: during the *RR* assistance the delay between the FD and its motor we found a delay of 190 ± 87 ms.

During the *RFF* assistance, the delay was 285 ± 92 ms for the FD activity.

C. Both controllers reduce human muscular effort during middle-high force levels of grasping

Fig. 5a shows the reaching task time-series of a representative subject, averaged across the repetitions of each force step: by looking at the APB muscle, it is possible to notice that the muscular effort is reduced, especially during the first 25% of the movement, when the participant initiates the reaching. The *RFF* algorithm assists more than the *RR*, which seems to follow the *NA* trend, in particular during the 10 N and the 15 N force steps. The reduction results have been further confirmed by the statistical analysis ($F_{3,6} = 3.33$, $p = 0.011$) at the population level (Fig. 5b), in which we found a significant reduction between the normalized sEMG activity of the APB muscle during the *NA* condition (10 N= 20.3 ± 4.1 of % MaxEMG, mean± SE; 15 N= $19.8 \pm 4.0\%$) and the two assistance conditions (*RR*: 10 N= $18.4 \pm 3.4\%$, $p = 0.001$; 15 N= $18.6 \pm 3.4\%$, $p < 0.001$. *RFF*: 10 N= $17.7 \pm 3.8\%$, $p < 0.001$; 15 N= $17.4 \pm 3.7\%$, $p < 0.001$.) No significant difference in measured muscle activity could be found while participants performed the 5 N force step trial, in which the APB activity was $19.4 \pm 4.0\%$, $18.8 \pm 3.5\%$ and $17.5 \pm 3.7\%$, respectively for *NA*, *RR* and *RFF*. Furthermore, no statistical differences are presented between the two controllers in assisting the APB muscle. Similar trends can be observed by looking at the FD muscle (Fig. 5) in which we found significant difference between the no assistance condition and the two controllers ($F_{3,6} = 33.6$, $p < 0.005$) for the 10 N force step (*NA*=$30.5 \pm 6.2\%$; *RR*=$23.3 \pm 4.5\%$, $p < 0.001$; *RFF*=$24.7 \pm 4.6\%$, $p = 0.001$) and the 15 N force step (*NA*=$31.0 \pm 6.2\%$; *RR*=$23.3 \pm 4.3\%$, $p < 0.001$; *RFF*=$24.9 \pm 4.8\%$, $p < 0.001$). As in the case of the APB muscle, the two controllers provided the same assistance on the FD, and they did not show significant difference with the no assistance condition for the lowest force step (5 N), in which the FD activity was $30.2 \pm 5.8\%$ during *NA* condition, $24.8 \pm 4.8\%$ during the *RR* assistance and $26.3 \pm 5.1\%$ during the *RFF*.

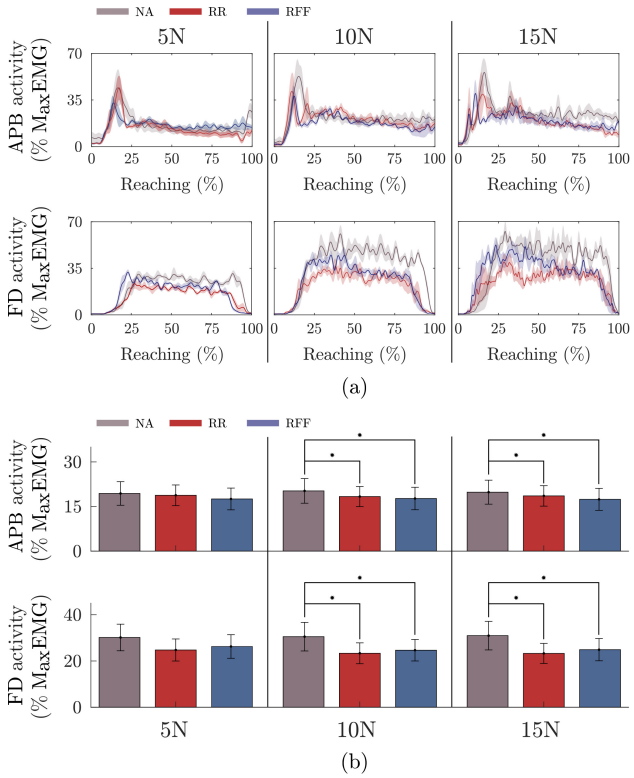

Fig. 5. *EMG analysis*. **a**: muscular activities of a typical participant during reaching task at different force steps, averaged across the five repetitions (mean ± sd): 5 N (left), 10 N (centre), and 15 N (right). Grey line represents NA condition, red and blue lines are respectively the trials performed during the assistance driven by the ridge regression (*RR*) and random Fourier feature (*RFF*) algorithms. **b** sEMG activity bar plot at the population level.

VII. Discussion

Wearable technologies have always been challenged by a variety of problems which are not only related to hardware design and ergonomics but also to the difficulty in delivering assistance to replicate lost or impaired motor functions. Providing assist-as-needed during task oriented grasping training is a particularly great challenge due to both the complexity of the anatomical structures as well as the high dexterity that characterizes it and provides humans with unmatched manual abilities. Although many solutions have been proposed in terms of hardware design, state-of-the-art controllers still leave several questions unanswered. In our contribution, we specifically aimed at providing a viable option to control actuated devices for hand assistance: we propose a rehabilitation platform that combines an actuated

soft glove driven by an intent detection system based upon machine learning applied to muscle activity and test it via a haptic handle device.

The work presents aspects of originality because it uses machine learning algorithms which are not merely classifying hand posture, but rather providing *a continuous estimation of the intended grasping force*, thus enabling the participant to precisely modulate the grasping interaction forces. While the mapping of EMG measurements to grasping forces through regression algorithms has been previously investigated [18][20], their use in compliant orthotic devices has never been explored in the past literature to the best of our knowledge. Our aim was to test the performance, considering two different machine learning approaches, as a first step towards assisted restorative grasping training. Both prediction algorithms show adequately accurate estimation of the exerted force, with no significant difference in their performance. This similarity is probably due to the fact that the EMG envelope shows a loose but inherent proportional relation to the grasping force. A more significant difference would likely be found if the systems were trained on more sEMG signals to operate a regression onto more assistance degrees of actuation. In such a case, the *RFF* algorithm could likely perform better, as it was shown in [22].

The two controllers did not show any significant difference in time response, with a delay between the sEMG onset and the motor actuation of about $0.2\,\mathrm{s}$: the importance of promptness in dynamic response is paramount in wearable devices in order to foster the wearer's sense of agency, which can be compromised in the presence of a delay between the user's motion intent (i.e. sEMG signals) and the device assistance. As demonstrated by Wen and colleagues [31], an action delay above $300\,\mathrm{ms}$ induces a lower sense of agency: a strong connection between the user and the robot, referred to as "embodiment", is a crucial aspect in clinical application, since it allows for more intuitive control [32] and most probably to better neuromotor recovery [33].

Both controllers reduced the activity of the two investigated muscles, APB and FD, during the middle (i.e. $10\,\mathrm{N}$) and high force steps (i.e. $15\,\mathrm{N}$): in particular, we saw higher reduction level ($\approx 50\%$) during the initial part of the task. This result further demonstrates the ability of the glove to react to the user's motion intent and to stabilize the hand in the desired force step. Should the glove's architecture remain unvaried, the ridge regression algorithm with no kernel would be preferable to RFF due to its reduced complexity and vulnerability to overfitting, and should be used in the future as the high-level controller.

Our study presents some limitations: the first one concerns the nature of the tested cohort of healthy participants, hence the performance of the two control schemes in people with upper extremity motor impairments is still an open question. Since in this preliminary work we focused on the feasibility of the platform, the next step will focus on testing such performances on patients (e.g. stroke or incomplete spinal cord injury) to clearly demonstrate that such approaches can be considered a viable option and concretely impact wearable assistive technology.

The second limitation concerns the soft glove: because the control loop takes as a setpoint the first time derivative of the machine learning-estimated desired hand closure, an overshoot of the target has often the effect of causing a release from the glove. This effect usually occurs when the muscle activity is not monotonically increasing during the reaching task, and it can thus be hard to prevent or predict. Integration of other low-level control architectures could be worth investigating. Finally, the lower reduction in muscular activity on the APB is likely due to the fact that the glove assists thumb flexion but not thumb abduction, which is normally performed when grasping a cylindrical object.

VIII. Conclusions

The human hand is a complex multi-joint system which enables the performance of a variety of tasks throughout our life: unfortunately, several diseases can affect its functionality. In the present work, we developed, for the first time, a demonstrator for a future rehabilitation platform that combines an EMG-driven machine learning soft glove with a haptic handle device aimed to restore grasping function through specific exercises. In this study we demonstrated a mostly compliant, closed-loop controlled actuated glove which can effectively use machine learning to provide assistance to a user during a force reaching task. While the effectiveness of the system was demonstrated in a scenario with a well-defined task-specific compliance matrix, its computation for an arbitrary task is a potentially non-trivial problem depending on the situation. Machine learning could provide the user with the possibility to easily switch between different levels of desired compliance by retraining the system, but an adequate integration of force or torque sensors in the glove design could bypass this problem while still allowing for closed-loop control. The training of the estimator may prove a non-trivial problem for users who are unable to achieve higher grasp forces. However, because the mapping is between muscular activity and intended forces, perhaps a recording procedure for impaired individuals could be envisioned, where the target is set to a higher level of compliance than during the testing tasks, with the assistive device bridging the gap. The main focus of the proposed intent estimators is incremental learning, rather than transfer learning. Ideally, training data should be gathered previous to all sessions from each user individually, and using another subject's data won't generally lead to good results.

References

[1] T. R. Tallis, *Hand: A Philosophical Inquiry Into Human Being*. Edinburgh University Press, 2019.

[2] J. R. Napier, "The prehensile movements of the human hand," *The Journal of Bone and Joint Surgery. British volume*, vol. 38, no. 4, pp. 902–913, 1956.

[3] I. A. Trail and A. N. Fleming, *Disorders of the Hand*. Springer, 2015.

[4] C.-Y. Chu and R. M. Patterson, "Soft robotic devices for hand rehabilitation and assistance: a narrative review," *Journal of Neuroengineering and Rehabilitation*, vol. 15, no. 1, pp. 1–14, 2018.

[5] C. L. Jones, F. Wang, R. Morrison, N. Sarkar, and D. G. Kamper, "Design and development of the cable actuated finger exoskeleton for hand rehabilitation following stroke," *IEEE/Asme Transactions on Mechatronics*, vol. 19, no. 1, pp. 131–140, 2012.

[6] L. Cappello, J. T. Meyer, K. C. Galloway, J. D. Peisner, R. Granberry, D. A. Wagner, S. Engelhardt, S. Paganoni, and C. J. Walsh, "Assisting hand function after spinal cord injury with a fabric-based soft robotic glove," *Journal of Neuroengineering and Rehabilitation*, vol. 15, no. 1, pp. 1–10, 2018.

[7] K. Nuckols, C. J. Hohimer, C. Glover, D. S. de Lucena, W. Moyo, D. Wagner, A. Cloutier, D. J. Lin, and C. J. Walsh, "Effects of a soft robotic glove using a high repetition protocol in chronic stroke: a pilot study," in *2020 8th IEEE RAS/EMBS International Conference for Biomedical Robotics and Biomechatronics (BioRob)*. IEEE, 2020, pp. 428–433.

[8] M. Xiloyannis, R. Alicea, A.-M. Georgarakis, F. L. Haufe, P. Wolf, L. Masia, and R. Riener, "Soft robotic suits: State of the art, core technologies, and open challenges," *IEEE Transactions on Robotics*, pp. 1–20, 2021.

[9] M. Santello, M. Flanders, and J. F. Soechting, "Postural hand synergies for tool use," *Journal of Neuroscience*, vol. 18, no. 23, pp. 10 105–10 115, 1998.

[10] A. C. McConnell, M. Vallejo, R. C. Moioli, F. L. Brasil, N. Secciani, M. P. Nemitz, C. P. Riquart, D. W. Corne, P. A. Vargas, and A. A. Stokes, "SOPHIA: soft orthotic physiotherapy hand interactive aid," *Frontiers in Mechanical Engineering*, vol. 3, p. 3, 2017.

[11] N. Cheng, K. S. Phua, H. S. Lai, P. K. Tam, K. Y. Tang, K. K. Cheng, R. C.-H. Yeow, K. K. Ang, C. Guan, and J. H. Lim, "Brain-computer interface-based soft robotic glove rehabilitation for stroke," *IEEE Transactions on Biomedical Engineering*, vol. 67, no. 12, pp. 3339–3351, 2020.

[12] H. K. Yap, B. W. Ang, J. H. Lim, J. C. Goh, and C.-H. Yeow, "A fabric-regulated soft robotic glove with user intent detection using EMG and RFID for hand assistive application," in *2016 IEEE International Conference on Robotics and Automation (ICRA)*. IEEE, 2016, pp. 3537–3542.

[13] C. G. Rose and M. K. O'Malley, "Hybrid rigid-soft hand exoskeleton to assist functional dexterity," *IEEE Robotics and Automation Letters*, vol. 4, no. 1, pp. 73–80, 2018.

[14] A. Dwivedi, L. Gerez, W. Hasan, C.-H. Yang, and M. Liarokapis, "A soft exoglove equipped with a wearable muscle-machine interface based on forcemyography and electromyography," *IEEE Robotics and Automation Letters*, vol. 4, no. 4, pp. 3240–3246, 2019.

[15] S. Cheon, D. Kim, S. Kim, B. B. Kang, J. Lee, H. Gong, S. Jo, K.-J. Cho, and J. Ahn, "Single EMG sensor-driven robotic glove control for reliable augmentation of power grasping," *IEEE Transactions on Medical Robotics and Bionics*, vol. 3, no. 1, pp. 179–189, 2020.

[16] P. Polygerinos, K. C. Galloway, S. Sanan, M. Herman, and C. J. Walsh, "EMG controlled soft robotic glove for assistance during activities of daily living," in *2015 IEEE International Conference on Rehabilitation Robotics (ICORR)*. IEEE, 2015, pp. 55–60.

[17] R. A. Bos, K. Nizamis, B. F. Koopman, J. L. Herder, M. Sartori, and D. H. Plettenburg, "A case study with SymbiHand: an sEMG-controlled electrohydraulic hand orthosis for individuals with Duchenne muscular dystrophy," *IEEE Transactions on Neural Systems and Rehabilitation Engineering*, vol. 28, no. 1, pp. 258–266, 2019.

[18] D. Yang, J. Zhao, Y. Gu, L. Jiang, and H. Liu, "Estimation of hand grasp force based on forearm surface EMG," in *2009 International Conference on Mechatronics and Automation*. IEEE, 2009, pp. 1795–1799.

[19] N. Parajuli, N. Sreenivasan, P. Bifulco, M. Cesarelli, S. Savino, V. Niola, D. Esposito, T. J. Hamilton, G. R. Naik, U. Gunawardana *et al.*, "Real-time EMG based pattern recognition control for hand prostheses: a review on existing methods, challenges and future implementation," *Sensors*, vol. 19, no. 20, p. 4596, 2019.

[20] R. Ma, L. Zhang, G. Li, D. Jiang, S. Xu, and D. Chen, "Grasping force prediction based on sEMG signals," *Alexandria Engineering Journal*, vol. 59, no. 3, pp. 1135–1147, 2020.

[21] A. Fougner, E. Scheme, A. D. Chan, K. Englehart, and Ø. Stavdahl, "Resolving the limb position effect in myoelectric pattern recognition," *IEEE Transactions on Neural Systems and Rehabilitation Engineering*, vol. 19, no. 6, pp. 644–651, 2011.

[22] A. Gijsberts, R. Bohra, D. Sierra González, A. Werner, M. Nowak, B. Caputo, M. A. Roa, and C. Castellini, "Stable myoelectric control of a hand prosthesis using non-linear incremental learning," *Frontiers in Neurorobotics*, vol. 8, p. 8, 2014.

[23] R. Alicea, M. Xiloyannis, D. Chiaradia, M. Barsotti, A. Frisoli, and L. Masia, "A soft, synergy-based robotic glove for grasping assistance," *Wearable Technologies*, vol. 2, 2021.

[24] H. J. Hermens, B. Freriks, C. Disselhorst-Klug, and G. Rau, "Development of recommendations for SEMG sensors and sensor placement procedures," *Journal of Electromyography and Kinesiology*, vol. 10, no. 5, pp. 361–374, 2000.

[25] A. E. Hoerl and R. W. Kennard, "Ridge regression: Biased estimation for nonorthogonal problems," *Technometrics*, vol. 12, pp. 55–67, 1970.

[26] J. Sherman and W. J. Morrison, "Adjustment of an inverse matrix corresponding to a change in one element of a given matrix," *The Annals of Mathematical Statistics*, vol. 21, no. 1, pp. 124–127, 1950.

[27] C. Saunders, A. Gammerman, and V. Vovk, "Ridge regression learning algorithm in dual variables," *15th International Conference on Machine Learning ICML '98*, 1998.

[28] A. Rahimi and B. Recht, "Random features for large-scale kernel machines," in *Proceedings of the 20th International Conference on Neural Information Processing Systems*, 2007, pp. 1177–1184.

[29] J. G. Ziegler, N. B. Nichols *et al.*, "Optimum settings for automatic controllers," *Transactions of the American Society of Mechanical Engineers*, vol. 64, no. 11, 1942.

[30] L. Masia, H. I. Krebs, P. Cappa, and N. Hogan, "Design and characterization of hand module for whole-arm rehabilitation following stroke," *IEEE/ASME Transactions on Mechatronics*, vol. 12, no. 4, pp. 399–407, 2007.

[31] W. Wen, A. Yamashita, and H. Asama, "The influence of action-outcome delay and arousal on sense of agency and the intentional binding effect," *Consciousness and Cognition*, vol. 36, pp. 87–95, 2015.

[32] M. Tsakiris, M. R. Longo, and P. Haggard, "Having a body versus moving your body: neural signatures of agency and body-ownership," *Neuropsychologia*, vol. 48, no. 9, pp. 2740–2749, 2010.

[33] M. Pazzaglia and M. Molinari, "The embodiment of assistive devices—from wheelchair to exoskeleton," *Physics of life reviews*, vol. 16, pp. 163–175, 2016.